



Sharif University of Technology

Scientia Iranica

Transactions B: Mechanical Engineering

www.sciencedirect.com



Analytical elastic–plastic study on flange wrinkling in deep drawing process

M. Kadkhodayan*, F. Moayyedean

Department of Mechanical Engineering, Ferdowsi University of Mashhad, Mashhad, P.O. Box 91775-1111, Iran

Received 4 July 2010; revised 12 November 2010; accepted 2 January 2011

KEYWORDS

Elastic wrinkling;
Plastic wrinkling;
Deep drawing process;
Large deflection;
Tresca yield criterion;
Bifurcation functional.

Abstract Based on the two-dimensional plane stress wrinkling model of an elastic–plastic annular plate and a bifurcation functional from Hill's general theory of uniqueness in polar coordinates, the critical conditions for the elastic and plastic wrinkling of the flange of a circular blank during the deep-drawing process are obtained to improve previous results of the literature. The influence of a blank-holder on wrinkling and on the number of waves generated can also be quantitatively predicted. A closed-form solution for the critical drawing stress is developed, based on the Tresca yield criterion, along with the assumption of perfectly plastic material. A nonlinear plastic stress field and the deformation theory of plasticity are used. It is demonstrated that using the large deflection theory for a strain tensor with neglecting nonlinear terms has the same result as the small deflection theory.

© 2011 Sharif University of Technology. Production and hosting by Elsevier B.V.

Open access under CC BY-NC-ND license.

1. Introduction

Wrinkling is considered one of the critical defects in deep drawing, together with tearing, springback and other geometric and surface defects. Contrary to fracturing, wrinkling can be treated as a recoverable defect, even when it develops during the deep drawing process.

However, for a deep drawing process, the wrinkling is not recoverable after forming. The wrinkle-waves become elastic–plastic in practice. Particularly, due to the geometric constraints of the die shoulder radius, the drawing force far exceeds the yield strength of the material, resulting in non-recoverable wrinkling waves.

Many researchers' efforts have been dedicated to predicting the occurrence, location and shape of the wrinkles. The work initiated from Hill's general theory of uniqueness and bifurcation [1] has been used by other researchers. Wrinkling occurs when the compressive stresses go beyond a certain

value during forming. In a deep-drawing operation, an initially flat round blank is drawn over a die by a cylindrical punch (see Figure 1). The annular part of the blank is subjected to a radial tensile stress, while in the circumferential direction, compressive stress is generated during drawing (see Figure 2). For particular dimensions of the drawing-tool and blank thickness, there is a critical blank diameter/thickness ratio, as critical stress causes elastic–plastic buckling in the annular part of the blank. This causes an undesirable mode of deformation to ensue with waves being produced in the flange (see Figure 3). This wrinkling can be prevented by employing a blank-holder, as shown in Figure 1 [2]. Many approaches have been made during past years to meet the requirements of press tool designers. Geckeler [3] early gave a mathematical analysis and two useful expressions for cases where no blank-holder was used. He showed that the critical stress at which buckling will occur is:

$$\sigma_{cr} = 0.46 \frac{E_0 t^2}{W^2},$$

where σ_{cr} is critical stress in the flange when buckling occurs, t the blank thickness, W the width of the flange and E_0 the buckling modulus determined by:

$$E_0 = \frac{4EP}{(\sqrt{E} + \sqrt{P})^2},$$

where E is the Young modulus and P the tangent modulus of the material, respectively. In addition, the number of waves during buckling of a flange is:

$$n = 1.65 \frac{r_m}{W},$$

* Corresponding author.

E-mail address: kadkhoda@um.ac.ir (M. Kadkhodayan).



Nomenclature

N_{ij}	force resultants
M_{ij}	couple resultants
κ_{ij}	curvature tensor
ε_{ij}^0	stretch strain tensor
F	bifurcation functional
u, v	in-plane displacement field
w	wrinkling displacement
ε_{ij}	Lagrangian strain
E	Young's modulus
ν	Poisson ratio
L_{ijkl}^e	elastic coefficient matrix
L_{ijkl}^{ep}	plastic coefficient matrix
f	yield criterion
Y	yield stress
U_0	density of strain energy
U	strain energy
W_E	external work
W	width of the flange
π	total potential energy
S	blankholder force
K	stiffness of the blankholder
t	thickness of the plate
a	inner radius of the flange
b	outer radius of the flange
n	wave number

where n is the number of waves and r_m the mean radius of the flange. Esser and Arend [4] developed an empirical equation to fit the obtained data from annealed copper, brass and mild steel. Their equation reduces to $b - a = 4.35t$, where b is the blank radius and a the inner radius of the flange. An outstanding approach by Baldwin and Howald [5] was developed in 1947 by means of applying Geckeler's equations to the prediction of limit reductions in diameter for given conditions of metal. In 1956, Geckeler's equations were extended by Senior [6]. In his solution, energy expended in the flange by circumferential stress was equated to the energy dissipated in the buckling of the flange. The method was applied for buckling under both constant load and spring-loaded blank-holders. Since he only used a one-dimensional buckling model, the flange was approximated as a number of linked struts, and a pressure distribution was assumed for the boundary condition at the inner edge that seems not to be very realistic. Comments on this work were made by Alexander [7]. Most previous work on this subject is thus based on the one-dimensional buckling model, so that those results can be expected to have a good approximation only when the width of the flange is small compared with the radius of the blank, that is $W = b - a \ll b$, or $\xi \ll 1$, where $\xi = 1 - m = 1 - \frac{a}{b}$, and $m = \frac{a}{b}$. Alternatively, Yu and Johnson [8] used the energy method in the elastic stability theory as a basis for plastic wrinkling analysis. They proposed an equation for balancing the work done by stresses induced in the flange, and the strain energy due to bending in the plastic wrinkling. According to their analysis, the onset of plastic wrinkling is governed by:

$$\sqrt{\frac{E_0 t}{Y b}} < \frac{3}{2} \sqrt{\frac{H(m, n)}{F^p(m, n)}},$$

where entities H and F^p are functions of the wave number and the flange dimension. The wave numbers computed from the above equation are lower than those from experimental results

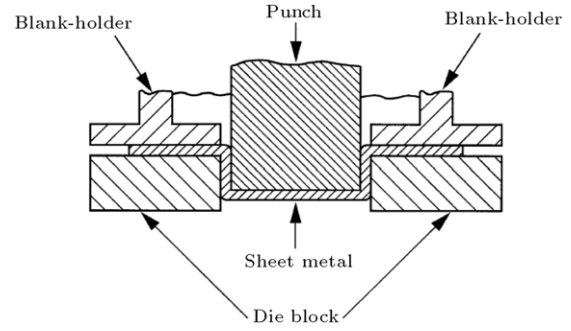


Figure 1: Deep drawing process with cylindrical punch.

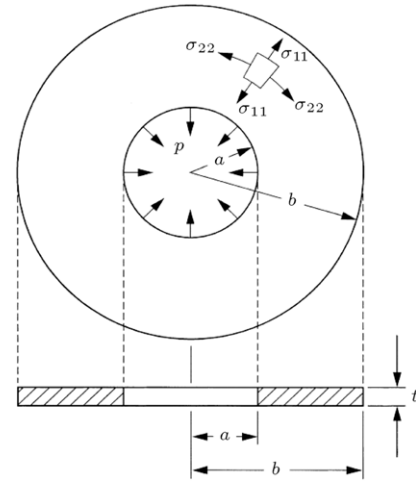


Figure 2: Model of flange as an annular plate with radial stress distribution at its inner edge.

and those obtained from Geckeler's and Senior's equations [3,6]. The reader is referred to the work done by Yu et al. [8,9] for further details of their approaches. Subsequently, Yossifon and Tirosh [10] extended the analysis to investigate fluid pressure as an additional energy term in their equation. All analyses reported so far are either based on a one-dimensional beam theory, which is too simplistic, or on a two-dimensional elastic-based rigid-plastic stability theory. The one-dimensional beam theory type of formulation, which ignores effects of shear stress and higher-order terms in the stability equation, cannot fully describe the flange wrinkling phenomena of a deep-drawn cup. The two-dimensional formulations have entirely relied on the elastic-based stability equation of plates. However, most investigators [6–9] simply replaced the Young modulus in buckling analysis, which is quite inadequate. Some researchers have also considered numerical solutions and therefore their work is far from analytical solutions [1,11,12]. The bifurcation functional was proposed by Hutchinson [13,14], based on Hill's general theory of uniqueness and bifurcation in elastic-plastic solids [15,16]. This functional [17–19] can be given as:

$$F = \iint (M_{ij}\kappa_{ij} + N_{ij}\varepsilon_{ij}^0 + N_{ij}w_{,i}w_{,j})ds. \quad (1)$$

After some changes, it may be written in the following form:

$$F(u, v, w) = \iint \left(\frac{t^3}{12} L_{ijkl}\kappa_{ij}\kappa_{kl} + tL_{ijkl}\varepsilon_{ij}^0\varepsilon_{kl}^0 + t\sigma_{ij}w_{,i}w_{,j} \right) ds, \quad (2a)$$

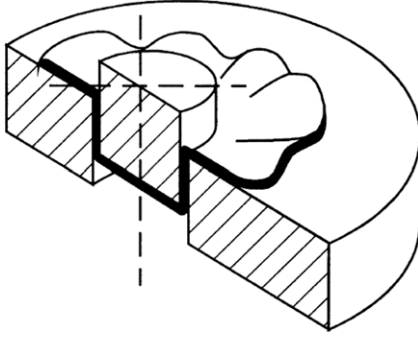


Figure 3: Generated waves in flange.

$$F = \iint \frac{t^3}{12} L_{ijkl} \kappa_{ij} \kappa_{kl} + \iint t L_{ijkl} \varepsilon_{ij}^0 \varepsilon_{kl}^0 ds + \iint t \sigma_{ij} w_{,i} w_{,j} ds. \quad (2b)$$

In this equation, s denotes the region of the middle surface where the wrinkles appear, u and v in-plane displacements, w the buckling displacement, t the thickness of the plate, N_{ij} the stress resultants, M_{ij} the stress couples (per unit width), κ_{ij} the bending strain (or the change of the curvature) tensor, and ε_{ij}^0 the stretch strain tensor. This bifurcation functional is the total energy required for wrinkling occurrence. In the right hand side of Eq. (1), the first term represents the bending energy ($i = j$) and twisting energy ($i \neq j$), the second term is the strain energy due to the membrane stresses and the third term may be interpreted as the potential energy of edge stress or the work done by the applied in-plane stresses in the middle surface. For all admissible displacement fields of u , v and w , if $F > 0$, then the solutions of the deformation are unique and bifurcation is not possible. In this case, to create wrinkles, the total potential of the system has to be increased. When $F = 0$, it corresponds to the critical conditions for wrinkles to occur for some non-zero displacement fields. Hence, the wrinkling criterion may be written as $F(u, v, w) = 0$ (not all $u, v = 0$ and $w = 0$).

The current study is based on a two-dimensional plane stress wrinkling model. An annular plate is studied using the bifurcation functional (see Eq. (1)) in the polar coordinate and in elastic-plastic cases with small/large deflection, as well as with/without the blank-holder. It examines and improves the results given by Geckeler [3] Senior [6] Yu and Johnson [8].

2. The elastic wrinkling of isotropic annular plates

2.1. Thin plate with small deflection

If the deflection, w , of a plate is small compared to its thickness, t , a very satisfactory approximate theory of bending can be developed by making the following assumptions:

1. There is no deformation in the middle plane of the plate, and any strain in the middle plane of the plate during bending can be neglected.
2. Points of a plate lying initially on a normal-to-the-middle plane of the plate remain on the normal-to-the middle surface of the plate after bending.
3. The normal stresses in the deflection transverse to the plate can be ignored.

Using these assumptions, all stress components can be expressed by deflection w of the plate, which is a function of the

two coordinates in the plane of the plate. If the external forces also act in the middle plane of the plate, the first assumption does not hold any more, and it is necessary to take into account the effect of the stresses acting in the middle plane of the plate on bending [20,21]. Because of the in-plane loading and small thickness of the plate, the problem can be considered as two-dimensional plane stress. When the coordinate system is set at the middle surface of the non-deformed (pre-buckled) plate, the material points in the plate are identified by coordinates r and θ lying at the middle surface of the un-deformed body, and the coordinate z normal to the middle surface. Therefore, the bending strain (or the change of the curvature), κ_{ij} , in the middle surface is created as:

$$\kappa_{ij} = -w_{,ij}, \quad (3)$$

where w is the buckling displacement normal to the middle surface of the plate. For annular plate and plane stress problems, we have:

$$\begin{cases} \kappa_{11} = -\frac{\partial^2 w}{\partial r^2}, \\ \kappa_{22} = -\frac{1}{r} \frac{\partial w}{\partial r} - \frac{1}{r^2} \frac{\partial^2 w}{\partial \theta^2}, \\ \kappa_{12} = -\frac{1}{r} \frac{\partial^2 w}{\partial r \partial \theta} + \frac{1}{r^2} \frac{\partial w}{\partial \theta}. \end{cases} \quad (4)$$

Then the Lagrangian strain tensor for any point inside the plate with distances z from the neutral plane can be defined as:

$$\varepsilon_{ij} = z \kappa_{ij}. \quad (5)$$

The stress resultants and stress couples (per unit width) are defined as:

$$\begin{cases} N_{ij} = \int_{-\frac{t}{2}}^{+\frac{t}{2}} \sigma_{ij} dz, \\ M_{ij} = \int_{-\frac{t}{2}}^{+\frac{t}{2}} \sigma_{ij} z dz. \end{cases} \quad (6)$$

The constitutive equation for an elastic solid is:

$$\sigma_{ij} = L_{ijkl}^e \varepsilon_{kl}. \quad (7)$$

This equation for the plane stress problems becomes:

$$\begin{Bmatrix} \sigma_{11} \\ \sigma_{22} \\ \tau_{12} \end{Bmatrix} = \begin{bmatrix} \frac{E}{1-\nu^2} & \frac{\nu E}{1-\nu^2} & 0 \\ \frac{\nu E}{1-\nu^2} & \frac{E}{1-\nu^2} & 0 \\ 0 & 0 & \frac{E}{2(1+\nu)} \end{bmatrix} \begin{Bmatrix} \varepsilon_{11} \\ \varepsilon_{22} \\ \gamma_{12} \end{Bmatrix}, \quad (8)$$

where E is the Young modulus of elasticity and ν is the Poisson ratio. By substituting Eq. (5) into Eq. (7) and putting the results into Eq. (6), the force and couple resultants are found as:

$$\begin{cases} N_{ij} = \int_{-\frac{t}{2}}^{+\frac{t}{2}} \sigma_{ij} dz = \int_{-\frac{t}{2}}^{+\frac{t}{2}} L_{ijkl}^e \kappa_{kl} z dz = 0, \\ M_{ij} = \int_{-\frac{t}{2}}^{+\frac{t}{2}} \sigma_{ij} z dz = \int_{-\frac{t}{2}}^{+\frac{t}{2}} L_{ijkl}^e \kappa_{kl} z^2 dz = \frac{t^3}{12} L_{ijkl}^e \kappa_{kl}. \end{cases} \quad (9)$$

Then, Eq. (1) for this case becomes:

$$\begin{aligned} F(w) &= \frac{1}{2} \int_0^{2\pi} \int_a^b \left(\frac{t^3}{12} L_{ijkl}^e \kappa_{ij} \kappa_{kl} + t \sigma_{ij} w_{,i} w_{,j} \right) r dr d\theta \\ &= \frac{1}{2} \int_0^{2\pi} \int_a^b \frac{t^3}{12} L_{ijkl}^e \kappa_{ij} \kappa_{kl} r dr d\theta \\ &\quad + \frac{1}{2} \int_0^{2\pi} \int_a^b t \sigma_{ij} w_{,i} w_{,j} r dr d\theta. \end{aligned} \quad (10)$$

If Eqs. (4) and (8) are inserted into the above functional, we will have:

$$F = \frac{1}{2} \int_0^{2\pi} \int_a^b \left\{ \frac{t^3}{12} \left[L_{1111}^e \left(\frac{\partial^2 w}{\partial r^2} \right)^2 + 2L_{1122}^e \left(\frac{\partial^2 w}{\partial r^2} \right) \left(\frac{1}{r} \frac{\partial w}{\partial r} + \frac{1}{r^2} \frac{\partial^2 w}{\partial \theta^2} \right) + L_{2222}^e \left(\frac{1}{r} \frac{\partial w}{\partial r} + \frac{1}{r^2} \frac{\partial^2 w}{\partial \theta^2} \right)^2 + 4L_{1212}^e \left(\frac{1}{r} \frac{\partial^2 w}{\partial r \partial \theta} - \frac{1}{r^2} \frac{\partial w}{\partial \theta} \right)^2 \right] \right\} r dr d\theta + \frac{1}{2} \int_0^{2\pi} \int_a^b \left\{ t \left[\sigma_r \left(\frac{\partial w}{\partial r} \right)^2 + \sigma_\theta \left(\frac{1}{r} \frac{\partial w}{\partial \theta} \right)^2 \right] \right\} r dr d\theta, \quad (11)$$

where the displacement, w , can be written as a function of the radial coordinate, r , and the polar angle, θ . Now it is assumed that the displacement field of the flange for a deep drawn cup has the following form [2,8]:

$$w(r, \theta) = c(r-a)(1 + \cos n\theta), \quad (12)$$

where c is a constant and n is the wave number. It is obvious that any admissible bifurcation mode in Eq. (12) satisfies the kinematical boundary condition, $w = 0$, at the inner edge of the flange for $r = a$, and the kinematical constraint condition $w(r, \theta) \geq 0$ for $a \leq r \leq b$. To obtain the critical load and the critical wave number using the functional, the pre-buckled elastic isotropic stress distribution in an annular plate subjected to radial stress, p , along its inner edge, can be found as [8]:

$$\begin{cases} \sigma_r = \frac{pa^2}{b^2 - a^2} \left(\frac{b^2}{r^2} - 1 \right), \\ \sigma_\theta = -\frac{pa^2}{b^2 - a^2} \left(1 + \frac{b^2}{r^2} \right). \end{cases} \quad (13)$$

By substituting Eqs. (12) and (13) into Eq. (11), taking $m = \frac{a}{b}$ and flexural rigidity $D = \frac{Et^3}{12(1-\nu^2)}$ and integrating the obtained result, it is found that:

$$F = \frac{\pi c^2 D}{2} G(m, n, \nu) + \frac{\pi c^2 b^2 t p}{2} H(m, n), \quad (14)$$

where:

$$\begin{cases} G(m, n, \nu) = \left[-\frac{m^2}{2} + 2m + \ln \left(\frac{1}{m} \right) - \frac{3}{2} \right] n^4 + \left[-(1-\nu)m^2 + 2(\ln(m) - m) + 3 - \nu \right] n^2 + 3 \ln \left(\frac{1}{m} \right), \\ H(m, n) = \frac{m^2}{m^2 - 1} \left\{ \left[\left(1 + \ln \left(\frac{1}{m} \right) \right) m^2 + \ln \left(\frac{1}{m} \right) - 1 \right] n^2 + 3 \left(-\frac{1}{2} m^2 + \ln(m) + \frac{1}{2} \right) \right\}. \end{cases} \quad (15)$$

Then condition $F = 0$ corresponds to the critical conditions for wrinkles to occur [13–15], and we have:

$$\frac{b^2 t}{D} p = -\frac{G(m, n, \nu)}{H(m, n)}. \quad (16)$$

Then if the following condition is satisfied:

$$\frac{b^2 t}{D} p > -\frac{G(m, n, \nu)}{H(m, n)}, \quad (17)$$

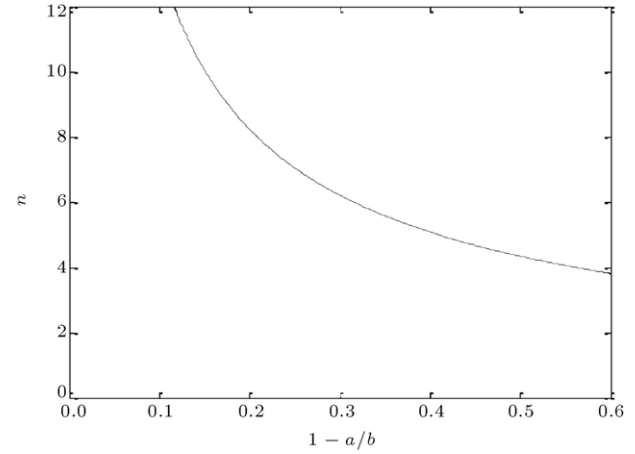


Figure 4: Number of waves for elastic wrinkling of flange.

wrinkling will occur. To determine the critical wave number, another condition has to be considered which is [17–19]:

$$\begin{cases} \frac{\partial F}{\partial n} = 0, \\ \text{or} \\ \frac{\partial p}{\partial n} = 0. \end{cases} \quad (18)$$

Eq. (14) has five roots for n , but only one of them is acceptable according to the specific range of $1 - \frac{a}{b}$. By taking $\nu = 0.3$, the variation of n versus $1 - \frac{a}{b}$ can be shown in Figure 4. It can be seen that obtained curves are quite close to Yu's result [8]. After finding n_{critical} from the root of $\frac{\partial p}{\partial n} = 0$ by inserting it into Eq. (16), the critical load, p_{critical} , can be obtained. Figure 5 displays the variation of $\frac{pb^2 t}{D}$ versus $1 - \frac{a}{b}$, along with a comparison with Yu's results [8]. For a thin annular plate of large diameter, the above elastic wrinkling model is possible, however, for a small diameter thick annular plate, p may cause yielding before buckling. For a thin annular plate in the elastic wrinkling case, we have the following:

$$(\sigma_r - \sigma_\theta)_{r=a} = p \frac{2b^2}{b^2 - a^2} = p \frac{2}{1 - m^2} < Y, \quad (19)$$

which may result in the following relation:

$$p < \frac{1 - m^2}{2} Y, \quad (20)$$

where Y is the yield stress of the material. Plastic yield occurs at the inner edge of the plate. Eq. (16) expresses a limitation for the application of determining the critical load. From Eqs. (16) and (20), this limitation can be written as:

$$\frac{b}{t} \geq \sqrt{-\frac{G(m, n)}{H(m, n)} \frac{E}{Y} \frac{1}{6(1-\nu^2)(1-m^2)}}. \quad (21)$$

For example, by taking $\frac{E}{Y} = 500$, $\nu = 0.3$ and $m = 0.6$, the computed results show that $-\frac{G(m, n)}{H(m, n)} = 59.1$ and $\frac{b}{t} \geq 92.0$. This means that when $\frac{b-a}{t} \geq 36.8$, elastic wrinkling occurs, and when $\frac{b-a}{t} \leq 36.8$, the tensile force, p , causes yielding before elastic wrinkling [8].

2.2. Thin plate with large deflection

In this case, in addition to κ_{ij} (the bending strain), the stretch strains, ε_{ij}^0 , have to be taken into account. Stretch strains, ε_{ij}^0 , in

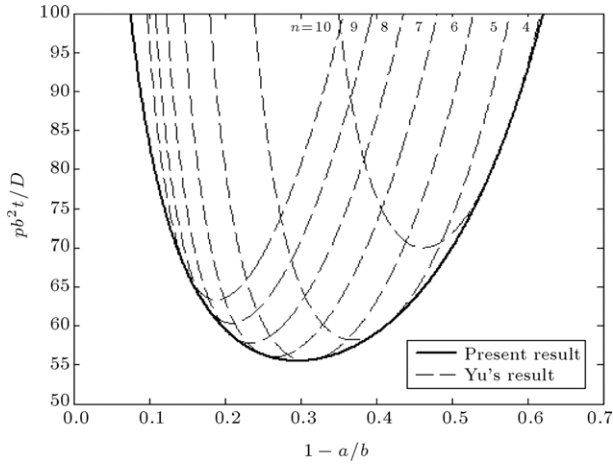


Figure 5: Critical load for elastic wrinkling of flange.

plane stress problems, and by neglecting nonlinear terms, are defined as:

$$\varepsilon_{ij}^0 = \frac{1}{2}(u_{i,j} + u_{j,i}). \quad (22)$$

In polar coordinates, the components of ε_{ij}^0 become:

$$\begin{cases} \varepsilon_{rr}^0 = \frac{\partial u}{\partial r}, \\ \varepsilon_{\theta\theta}^0 = \frac{u}{r} + \frac{1}{r} \frac{\partial v}{\partial \theta}, \\ \varepsilon_{r\theta}^0 = \frac{1}{2} \left(\frac{1}{r} \frac{\partial u}{\partial \theta} + \frac{\partial v}{\partial r} - \frac{v}{r} \right), \end{cases} \quad (23)$$

where u and v are in-plane displacements in the r and θ directions. Therefore, the Lagrangian strain tensor for any point inside the plate with distance z from the neutral plane can be defined as:

$$\varepsilon_{ij} = \varepsilon_{ij}^0 + z\kappa_{ij}. \quad (24)$$

By substituting Eq. (24) into Eq. (7) and putting the results into Eq. (9), the stress and couple resultants are found as:

$$\begin{cases} N_{ij} = \int_{-\frac{t}{2}}^{+\frac{t}{2}} \sigma_{ij} dz = \int_{-\frac{t}{2}}^{+\frac{t}{2}} L_{ijkl}^e (\varepsilon_{ij}^0 + z\kappa_{kl}) dz = t L_{ijkl}^e \varepsilon_{ij}^0, \\ M_{ij} = \int_{-\frac{t}{2}}^{+\frac{t}{2}} \sigma_{ij} z dz = \int_{-\frac{t}{2}}^{+\frac{t}{2}} L_{ijkl}^e (\varepsilon_{ij}^0 + z\kappa_{kl}) z dz = \frac{t^3}{12} L_{ijkl}^e \kappa_{kl}. \end{cases} \quad (25)$$

Then, Eq. (1) for this case becomes:

$$\begin{aligned} F(u, v, w) &= \frac{1}{2} \int_0^{2\pi} \int_a^b \left(\frac{t^3}{12} L_{ijkl}^e \kappa_{ij} \kappa_{kl} + t L_{ijkl}^e \varepsilon_{ij}^0 \varepsilon_{kl}^0 \right) \\ &\quad + t \sigma_{ij} w_{,i} w_{,j} r dr d\theta \\ &= \frac{1}{2} \int_0^{2\pi} \int_a^b \frac{t^3}{12} L_{ijkl}^e \kappa_{ij} \kappa_{kl} r dr d\theta \\ &\quad + \frac{1}{2} \int_0^{2\pi} \int_a^b t L_{ijkl}^e \varepsilon_{ij}^0 \varepsilon_{kl}^0 r dr d\theta \\ &\quad + \frac{1}{2} \int_0^{2\pi} \int_a^b t \sigma_{ij} w_{,i} w_{,j} r dr d\theta. \end{aligned} \quad (26)$$

By inserting Eqs. (4) and (23), the functional is obtained as:

$$\begin{aligned} F &= \frac{1}{2} \int_0^{2\pi} \int_a^b \left\{ \frac{t^3}{12} \left[L_{1111}^e \left(\frac{\partial^2 w}{\partial r^2} \right)^2 \right. \right. \\ &\quad + 2L_{1122}^e \left(\frac{\partial^2 w}{\partial r^2} \right) \left(\frac{1}{r} \frac{\partial w}{\partial r} + \frac{1}{r^2} \frac{\partial^2 w}{\partial \theta^2} \right) \\ &\quad + L_{2222}^e \left(\frac{1}{r} \frac{\partial w}{\partial r} + \frac{1}{r^2} \frac{\partial^2 w}{\partial \theta^2} \right)^2 \\ &\quad + 4L_{1212}^e \left(\frac{1}{r} \frac{\partial^2 w}{\partial r \partial \theta} - \frac{1}{r^2} \frac{\partial w}{\partial \theta} \right)^2 \left. \right] r dr d\theta \\ &\quad + \frac{1}{2} \int_0^{2\pi} \int_a^b \left\{ t \left[L_{1111}^e \left(\frac{\partial u}{\partial r} \right)^2 \right. \right. \\ &\quad + 2L_{1122}^e \left(\frac{\partial u}{\partial r} \right) \left(\frac{u}{r} + \frac{1}{r} \frac{\partial v}{\partial \theta} \right) \\ &\quad + L_{2222}^e \left(\frac{u}{r} + \frac{1}{r} \frac{\partial v}{\partial \theta} \right)^2 \\ &\quad + L_{1212}^e \left(\frac{1}{r} \frac{\partial u}{\partial \theta} + \frac{\partial v}{\partial \theta} - \frac{v}{r} \right)^2 \left. \right] r dr d\theta \\ &\quad + \frac{1}{2} \int_0^{2\pi} \int_a^b \left\{ t \left[\sigma_r \left(\frac{\partial w}{\partial r} \right)^2 + \sigma_\theta \left(\frac{1}{r} \frac{\partial w}{\partial \theta} \right)^2 \right] r dr d\theta. \right. \end{aligned} \quad (27)$$

The first and third integrals are exactly the same as Eq. (11), but the second one has to be found. For calculating the second integral, it may be assumed that the displacements, u and v , can be expressed as a function of the radial coordinate, r , and the polar angle, θ , as follows [22,23]:

$$\begin{cases} u(r, \theta) = dr \cos n\theta, \\ v(r, \theta) = er \sin n\theta, \end{cases} \quad (28)$$

where d and e are constants. It is obvious that any admissible bifurcation mode in Eq. (28) satisfies the kinematical boundary conditions, $u = v = 0$, at the center of the plate ($r = 0$), $u \neq 0$ and $v \neq 0$ at the inner edge $r = a$, and the kinematical constraint condition $u(r, \theta) \geq 0$ and $v(r, \theta) \geq 0$ for $a \leq r \leq b$. To obtain the critical load and wave number, the pre-buckled elastic isotropic stress distribution in an annular plate subjected to radial stress, p , along its inner edge, is investigated. The stress distribution for large deflection before wrinkling is the same as Eq. (13) because of the symmetry of the geometry before wrinkling ($v = 0$ and $\frac{\partial}{\partial \theta} = 0$). By substituting Eq. (28) into the second integral of Eq. (27), it is created that:

$$\begin{aligned} F &= \frac{\pi c^2 D}{2} G(m, n, v) + \frac{\pi t E b^2}{8(1 - \nu^2)} \{ Q(m, n, v) d^2 \\ &\quad + R(m, n, v) de + S(m, n) e^2 \} + \frac{\pi c^2 b^2 t p}{2} H(m, n), \end{aligned} \quad (29)$$

where:

$$\begin{cases} Q(m, n, v) = (1 - m^2)[(1 - \nu)n^2 + 4(1 + \nu)], \\ R(m, n, v) = 4(1 - m^2)(1 + \nu)n, \\ S(m, n) = 2(1 - m^2)n^2. \end{cases} \quad (30)$$

It is more convincing to write the above functional in the following matrix form:

$$F = \{c \quad d \quad e\} \begin{bmatrix} M_{11} & 0 & 0 \\ 0 & M_{22} & M_{23} \\ 0 & M_{32} & M_{33} \end{bmatrix} \begin{Bmatrix} c \\ d \\ e \end{Bmatrix}, \quad (31)$$

where:

$$\begin{cases} M_{11} = \frac{\pi D}{2} G(m, n, \nu) + \frac{\pi b^2 t p}{2} H(m, n), \\ M_{22} = \frac{\pi t E b^2}{8(1-\nu^2)} Q(m, n, \nu), \\ M_{23} = M_{32} = \frac{1}{2} \frac{\pi t E b^2}{8(1-\nu^2)} R(m, n, \nu), \\ M_{33} = \frac{\pi t E b^2}{8(1-\nu^2)} S(m, n). \end{cases} \quad (32)$$

Therefore, the two conditions to determine the critical number of waves and critical load are [17–19]:

$$\begin{cases} F = 0 & \text{or} & \text{Det}(M_{ij}) = 0, \\ \frac{\partial F}{\partial n} = 0 & \text{or} & \frac{\partial [\text{Det}(M_{ij})]}{\partial n} = 0. \end{cases} \quad (33)$$

The first condition in Eq. (33) yields to:

$$\text{Det}(M_{ij}) = M_{11}(M_{22}M_{33} - M_{23}^2) = 0,$$

because:

$$(M_{22}M_{33} - M_{23}^2) \neq 0,$$

the condition $\text{Det}(M_{ij}) = 0$ yields to $M_{11} = 0$, which is exactly the same condition as in the small deflection theory. Hence, it may be observed that the results for the critical number of waves and the critical load are exactly the same as the small deflection with neglecting nonlinear terms in stretching tensor ε_{ij}^0 .

3. The plastic wrinkling of isotropic annular plates (without a blank-holder)

The general validity of the deformation theory in plasticity is limited to the monotonically increasing loading where:

1. The stress components are increased nearly proportionally in a loading process, known as proportional loading;
2. No unloading occurs. In this case, it can be assumed that the stress state, σ_{ij} , determines the total strain and plastic strain state, ε_{ij} and ε_{ij}^p , as long as the plastic deformation continues [24–27].

When an annular plate is subjected to an in-plane loading, these conditions are nearly satisfied; hence, it is easier to use the deformation theory rather than the incremental theory of plasticity. The constitutive equation from the deformation theory for a solid in 3D problems is:

$$\sigma_{ij} = L_{ijkl}^{\text{ep}} \varepsilon_{kl}, \quad (34)$$

where L_{ijkl}^{ep} , for a perfectly plastic material, can be determined by [24–27]:

$$L_{ijkl}^{\text{ep}} = L_{ijkl}^e - \frac{L_{ijkl}^e \frac{\partial f}{\partial \sigma_{mn}} \frac{\partial f}{\partial \sigma_{pq}} L_{pqkl}^e}{\frac{\partial f}{\partial \sigma_{rs}} L_{rstu}^e \frac{\partial f}{\partial \sigma_{tu}}}, \quad (35)$$

where f is a proper yield criterion, according to the problem. In the current study, the Tresca yield criterion is employed to obtain L_{ijkl}^{ep} , and we have $f = \sigma_r - \sigma_\theta - Y = 0$. Then, by expanding Eq. (34) for $i, j, k, l = 1, 2, 3$, using Eq. (35) and the Tresca yield criterion for L_{ijkl}^{ep} and, also, assuming plane stress conditions, $\sigma_{33} = \sigma_{13} = \sigma_{23} = 0$, the constitutive equation

for the deformation theory of plasticity may be obtained in the following simple form:

$$\begin{Bmatrix} \sigma_{11} \\ \sigma_{22} \\ \tau_{12} \end{Bmatrix} = \begin{bmatrix} \frac{E}{2(1-\nu)} & \frac{E}{2(1-\nu)} & 0 \\ \frac{E}{2(1-\nu)} & \frac{E}{2(1-\nu)} & 0 \\ 0 & 0 & \frac{E}{2(1+\nu)} \end{bmatrix} \begin{Bmatrix} \varepsilon_{11} \\ \varepsilon_{22} \\ \gamma_{12} \end{Bmatrix}. \quad (36)$$

3.1. Thin plate with small deflection

If the initial elastic buckling does not occur and the annular plate is in a fully plastic state [9] while deep-drawing is proceeding, Eq. (1) becomes:

$$\begin{aligned} F(w) &= \frac{1}{2} \int_0^{2\pi} \int_a^b \left(\frac{t^3}{12} L_{ijkl}^{\text{ep}} \kappa_{ij} \kappa_{kl} + t \sigma_{ij} w_{,i} w_{,j} \right) r dr d\theta \\ &= \frac{1}{2} \int_0^{2\pi} \int_a^b \frac{t^3}{12} L_{ijkl}^{\text{ep}} \kappa_{ij} \kappa_{kl} r dr d\theta \\ &\quad + \frac{1}{2} \int_0^{2\pi} \int_a^b t \sigma_{ij} w_{,i} w_{,j} r dr d\theta. \end{aligned} \quad (37)$$

By the same procedure as before, it takes the form below:

$$\begin{aligned} F &= \frac{1}{2} \int_0^{2\pi} \int_a^b \left\{ \frac{t^3}{12} \left[L_{1111}^{\text{ep}} \left(\frac{\partial^2 w}{\partial r^2} \right)^2 \right. \right. \\ &\quad + 2L_{1122}^{\text{ep}} \left(\frac{\partial^2 w}{\partial r^2} \right) \left(\frac{1}{r} \frac{\partial w}{\partial r} + \frac{1}{r^2} \frac{\partial^2 w}{\partial \theta^2} \right) \\ &\quad + L_{2222}^{\text{ep}} \left(\frac{1}{r} \frac{\partial w}{\partial r} + \frac{1}{r^2} \frac{\partial^2 w}{\partial \theta^2} \right)^2 \\ &\quad \left. \left. + 4L_{1212}^{\text{ep}} \left(\frac{1}{r} \frac{\partial^2 w}{\partial r \partial \theta} - \frac{1}{r^2} \frac{\partial w}{\partial \theta} \right)^2 \right] \right\} r dr d\theta \\ &\quad + \frac{1}{2} \int_0^{2\pi} \int_a^b \left\{ t \left[\sigma_r \left(\frac{\partial w}{\partial r} \right)^2 + \sigma_\theta \left(\frac{1}{r} \frac{\partial w}{\partial \theta} \right)^2 \right] \right\} r dr d\theta. \end{aligned} \quad (38)$$

The displacement, w , may be expressed as a function of the radial coordinate, r , and the polar angle, θ , as Eq. (12) [2,8]. To obtain the critical wave number and the critical load, pre-buckled plastic isotropic stress distribution in an annular plate subjected to radial stress, p , along its inner edge, using the Tresca yield criterion, can be used [2,8,24]:

$$\begin{cases} \sigma_r = Y \ln \left(\frac{b}{r} \right) > 0, \\ \sigma_\theta = Y \left[\ln \left(\frac{b}{r} \right) - 1 \right] < 0. \end{cases} \quad (39)$$

By substituting Eqs. (12) and (39) into Eq. (38), and taking $m = \frac{a}{b}$, integrating the equation yields:

$$F = \frac{t^3 c^2 E \pi}{96(1-\nu^2)} G^{\text{ep}}(m, n, \nu) + \frac{t \pi b^2 c^2 Y}{8} H^{\text{ep}}(m, n), \quad (40)$$

where:

$$\begin{cases} G^{ep}(m, n, \nu) = (1 + \nu) \left[-m^2 + 4m + 2 \ln\left(\frac{1}{m}\right) - 3 \right] n \\ \quad + 4 \left[-(1 - \nu)m^2 + (1 + \nu)(\ln(m) - m) + 2 \right] n^2 \\ \quad + 6 \ln\left(\frac{1}{m}\right) (1 + \nu), \\ H^{ep}(m, n) = 2 \left\{ \left[\left(\ln\left(\frac{1}{m}\right) \right)^2 + \ln\left(\frac{1}{m}\right) \right. \right. \\ \quad \left. \left. + \frac{1}{2} \right] m^2 - \frac{1}{2} \right\} n^2 \\ \quad + 3[(2 \ln(m) - 1)m^2 + 1]. \end{cases} \quad (41)$$

Then, condition $F = 0$ corresponds to the critical condition for wrinkles to occur which is:

$$Y = -\frac{E}{12(1 - \nu^2)} \frac{t^2}{b^2} \frac{G^{ep}(m, n, \nu)}{H^{ep}(m, n)}, \quad (42)$$

To compare with other results, Eq. (42) can be written in the following form:

$$\sqrt{\frac{E}{Y}} \frac{t}{b} = \sqrt{-12(1 - \nu^2) \frac{H^{ep}(m, n)}{G^{ep}(m, n, \nu)}}. \quad (43)$$

When:

$$\sqrt{\frac{E}{Y}} \frac{t}{b} < \sqrt{-12(1 - \nu^2) \frac{H^{ep}(m, n)}{G^{ep}(m, n, \nu)}}, \quad (44)$$

wrinkling will occur.

To determine the critical wave number, the following conditions have to be considered:

$$\begin{cases} \frac{\partial F}{\partial n} = 0, \\ \text{or} \\ \frac{\partial Y}{\partial n} = 0. \end{cases} \quad (45)$$

Eq. (45) has five roots for n but only one of them can be acceptable in the specific range of $1 - \frac{a}{b}$. Then, by taking $\nu = 0.3$, the variation of n versus $1 - \frac{a}{b}$ and its comparison with Yu's and experimental results is shown in Figure 6 [8]. When n_{critical} is known, it can be substituted into Eq. (23), and Y_{critical} can be found. Figure 7 shows the variation of $\sqrt{\frac{E}{Y}} \frac{t}{b}$ versus $1 - \frac{a}{b}$ along with a comparison with other results [8].

3.2. Thin plate with large deflection

Functional 1 for this case becomes:

$$\begin{aligned} F(u, v, w) &= \frac{1}{2} \int_0^{2\pi} \int_a^b \left(\frac{t^3}{12} L_{ijkl}^{ep} \kappa_{ij} \kappa_{kl} \right. \\ &\quad \left. + t L_{ijkl}^{ep} \varepsilon_{ij}^0 \varepsilon_{kl}^0 + t \sigma_{ij} w_{,i} w_{,j} \right) r dr d\theta \\ &= \frac{1}{2} \int_0^{2\pi} \int_a^b \frac{t^3}{12} L_{ijkl}^{ep} \kappa_{ij} \kappa_{kl} r dr d\theta \\ &\quad + \frac{1}{2} \int_0^{2\pi} \int_a^b t L_{ijkl}^{ep} \varepsilon_{ij}^0 \varepsilon_{kl}^0 r dr d\theta \\ &\quad + \frac{1}{2} \int_0^{2\pi} \int_a^b t \sigma_{ij} w_{,i} w_{,j} r dr d\theta. \end{aligned} \quad (46)$$

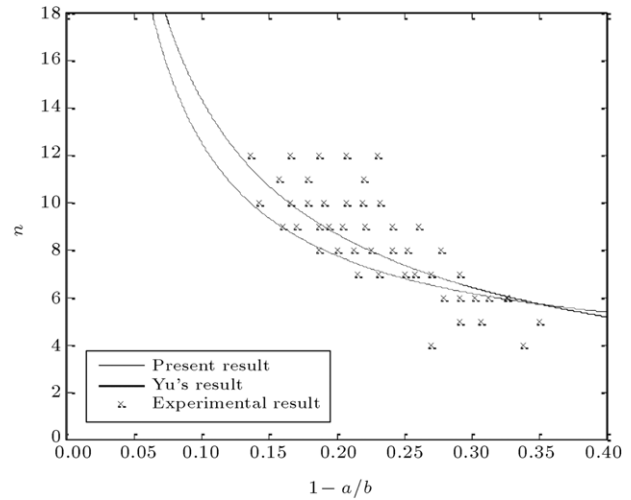


Figure 6: Number of generated waves in plastic flange wrinkling of annular plate.

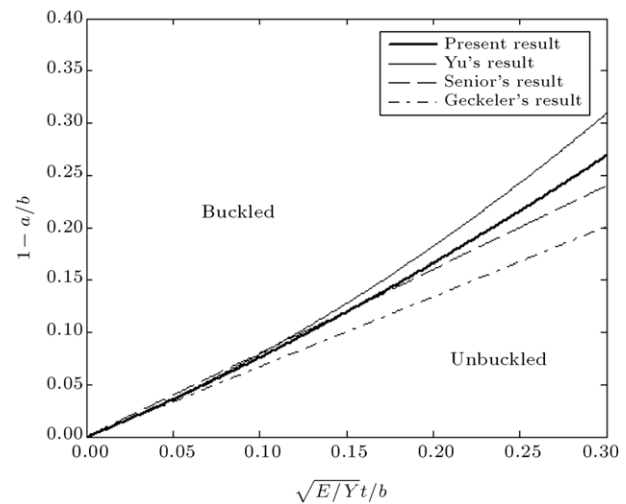


Figure 7: Onset of plastic wrinkling for flange.

With a similar procedure, it is obtained that:

$$\begin{aligned} F &= \frac{1}{2} \int_0^{2\pi} \int_a^b \left\{ \frac{t^3}{12} \left[L_{1111}^{ep} \left(\frac{\partial^2 w}{\partial r^2} \right)^2 \right. \right. \\ &\quad + 2L_{1122}^{ep} \left(\frac{\partial^2 w}{\partial r^2} \right) \left(\frac{1}{r} \frac{\partial w}{\partial r} + \frac{1}{r^2} \frac{\partial^2 w}{\partial \theta^2} \right) \\ &\quad + L_{2222}^{ep} \left(\frac{1}{r} \frac{\partial w}{\partial r} + \frac{1}{r^2} \frac{\partial^2 w}{\partial \theta^2} \right)^2 \\ &\quad \left. + 4L_{1212}^{ep} \left(\frac{1}{r} \frac{\partial^2 w}{\partial r \partial \theta} - \frac{1}{r^2} \frac{\partial w}{\partial \theta} \right)^2 \right\} r dr d\theta \\ &\quad + \frac{1}{2} \int_0^{2\pi} \int_a^b \left\{ t \left[L_{1111}^{ep} \left(\frac{\partial u}{\partial r} \right)^2 \right. \right. \\ &\quad + 2L_{1122}^{ep} \left(\frac{\partial u}{\partial r} \right) \left(\frac{u}{r} + \frac{1}{r} \frac{\partial v}{\partial \theta} \right) \\ &\quad \left. + L_{2222}^{ep} \left(\frac{u}{r} + \frac{1}{r} \frac{\partial v}{\partial \theta} \right)^2 \right] L_{1212}^{ep} \end{aligned}$$

$$\times \left(\frac{1}{r} \frac{\partial u}{\partial \theta} + \frac{\partial v}{\partial \theta} - \frac{v}{r} \right)^2 \Bigg] \Bigg\} r dr d\theta$$

$$+ \frac{1}{2} \int_0^{2\pi} \int_a^b \left\{ t \left[\sigma_r \left(\frac{\partial w}{\partial r} \right)^2 + \sigma_\theta \left(\frac{1}{r} \frac{\partial w}{\partial \theta} \right)^2 \right] \right\} r dr d\theta. \quad (47)$$

Similar to the large deflection case in elastic wrinkling, it is enough to calculate only the second integration, because the first and third ones are exactly the same as the small deflection in Eq. (38). It is assumed that displacements u and v have forms like Eq. (28). Then the above functional takes the form below:

$$F = \frac{t^3 c^2 E \pi}{96(1-\nu^2)} G^{ep}(m, n, \nu) + \frac{\pi t E b^2}{8(1-\nu^2)} \{ Q^{ep}(m, n, \nu) d^2$$

$$+ R^{ep}(m, n, \nu) d e + S^{ep}(m, n, \nu) e^2 \} + \frac{\pi c^2 b^2 t p}{2} H(m, n), \quad (48)$$

where:

$$\begin{cases} Q^{ep}(m, n, \nu) = (1-m^2)[(1-\nu)n^2 + 4(1+\nu)], \\ R^{ep}(m, n, \nu) = 4(1+\nu)(1-m^2)n, \\ S^{ep}(m, n, \nu) = (1-m^2)(1+\nu)n^2. \end{cases} \quad (49)$$

The functional becomes:

$$F = \begin{bmatrix} c & d & e \end{bmatrix} \begin{bmatrix} M_{11} & 0 & 0 \\ 0 & M_{22} & M_{23} \\ 0 & M_{32} & M_{33} \end{bmatrix} \begin{Bmatrix} c \\ d \\ e \end{Bmatrix}, \quad (50)$$

where:

$$\begin{cases} M_{11} = \frac{t^3 E \pi}{96(1-\nu^2)} G^{ep}(m, n, \nu) + \frac{\pi b^2 t Y}{8} H^{ep}(m, n), \\ M_{22} = \frac{\pi t E b^2}{8(1-\nu^2)} Q^{ep}(m, n, \nu), \\ M_{23} = M_{32} = \frac{1}{2} \frac{\pi t E b^2}{8(1-\nu^2)} R^{ep}(m, n, \nu), \\ M_{33} = \frac{\pi t E b^2}{8(1-\nu^2)} S^{ep}(m, n, \nu). \end{cases} \quad (51)$$

In this case, also the results for the critical number of waves and the critical load are exactly the same as those obtained from the small deflection theory when nonlinear terms in the stretching tensor, ε_{ij}^0 , are neglected.

4. Plastic wrinkling of isotropic annular plates (with a blank-holder)

4.1. Thin plate with small deflection

Functional 1 in this case becomes [8]:

$$F(w) = \frac{1}{2} \int_0^{2\pi} \int_a^b \left(\frac{t^3}{12} L_{ijkl}^{ep} \kappa_{ij} \kappa_{kl} + t \sigma_{ij} w_{,i} w_{,j} \right) r dr d\theta$$

$$+ \frac{1}{2} K w_{\max}^2 = \frac{1}{2} \int_0^{2\pi} \int_a^b \frac{t^3}{12} L_{ijkl}^{ep} \kappa_{ij} \kappa_{kl} r dr d\theta$$

$$+ \frac{1}{2} \int_0^{2\pi} \int_a^b t \sigma_{ij} w_{,i} w_{,j} r dr d\theta + \frac{1}{2} K w_{\max}^2, \quad (52)$$

where K is the stiffness of the blankholder. If it is assumed that the blankholder force per unit area is S , then we have [8]:

$$S = K \pi (b^2 - a^2). \quad (53)$$

Since the maximum deflection is:

$$w_{\max} = c(r-a)(1+\cos n\theta) \Big|_{\substack{r=b \\ \theta=0}} = 2c(b-a). \quad (54)$$

Then the energy stored in the spring-type blankholder is obtained as:

$$\frac{1}{2} K w_{\max}^2 = \frac{S}{2\pi(b^2-a^2)} 4c^2(b-a)^2 = \frac{2}{\pi} c^2 S \frac{1-m}{1+m}. \quad (55)$$

In this case, the functional becomes:

$$F = \frac{1}{2} \int_0^{2\pi} \int_a^b \left\{ \frac{t^3}{12} \left[L_{1111}^{ep} \left(\frac{\partial^2 w}{\partial r^2} \right)^2 \right. \right.$$

$$+ 2L_{1122}^{ep} \left(\frac{\partial^2 w}{\partial r^2} \right) \left(\frac{1}{r} \frac{\partial w}{\partial r} + \frac{1}{r^2} \frac{\partial^2 w}{\partial \theta^2} \right)$$

$$+ L_{2222}^{ep} \left(\frac{1}{r} \frac{\partial w}{\partial r} + \frac{1}{r^2} \frac{\partial^2 w}{\partial \theta^2} \right)^2$$

$$+ 4L_{1212}^{ep} \left(\frac{1}{r} \frac{\partial^2 w}{\partial r \partial \theta} - \frac{1}{r^2} \frac{\partial w}{\partial \theta} \right)^2 \Bigg] \Bigg\} r dr d\theta$$

$$+ \frac{1}{2} \int_0^{2\pi} \int_a^b \left\{ t \left[\sigma_r \left(\frac{\partial w}{\partial r} \right)^2 + \sigma_\theta \left(\frac{1}{r} \frac{\partial w}{\partial \theta} \right)^2 \right] \right\} r dr d\theta$$

$$+ \frac{2}{\pi} c^2 S \frac{1-m}{1+m}. \quad (56)$$

The first and second integrations of Eq. (56) are exactly the same as Eq. (47); then F becomes:

$$F = \frac{t^3 c^2 E \pi}{96(1-\nu^2)} G^{ep}(m, n, \nu) + \frac{t \pi b^2 c^2 Y}{8} H^{ep}(m, n)$$

$$+ \frac{2}{\pi} c^2 S \frac{1-m}{1+m}. \quad (57)$$

The critical condition for plastic buckling is $F = 0$, which results in:

$$Y = - \frac{\frac{G^{ep}}{4} + \left(\frac{2}{\pi} \right)^2 \frac{S}{D} \frac{1-m}{1+m}}{3 \left(\frac{b}{t} \right)^2 \frac{(1-\nu^2)}{E} H^{ep}}. \quad (58)$$

If it is assumed $\psi = \frac{S}{D}$, then the following relation is found:

$$\sqrt{\frac{E}{Y} \frac{t}{b}} = \sqrt{-3(1-\nu^2) \frac{H^{ep}}{\frac{G^{ep}}{4} + \left(\frac{2}{\pi} \right)^2 \psi \frac{1-m}{1+m}}}, \quad (59)$$

when:

$$\sqrt{\frac{E}{Y} \frac{t}{b}} < \sqrt{-3(1-\nu^2) \frac{H^{ep}}{\frac{G^{ep}}{4} + \left(\frac{2}{\pi} \right)^2 \psi \frac{1-m}{1+m}}}, \quad (60)$$

wrinkling will occur. Again, and to determine the critical wave number, the following conditions have to be considered as follows:

$$\begin{cases} \frac{\partial F}{\partial n} = 0, \\ \text{or} \\ \frac{\partial Y}{\partial n} = 0. \end{cases} \quad (61)$$

Eq. (61) has five roots for n , but only one of them is logical in a specific range of $1 - \frac{a}{b}$. By taking $\nu = 0.3$ and $\psi = 4000$, the variation of n with $1 - \frac{a}{b}$ is in Figure 8. After finding n_{critical} , by substituting it into Eq. (59), Y_{critical} can also be found.

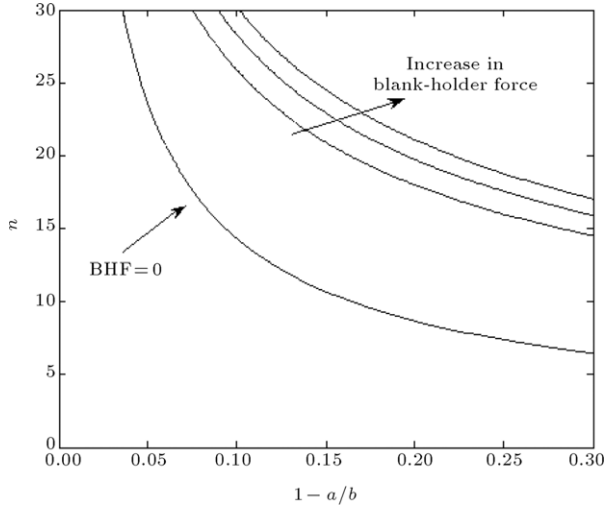


Figure 8: Number of generated waves in the flange for different BHF.

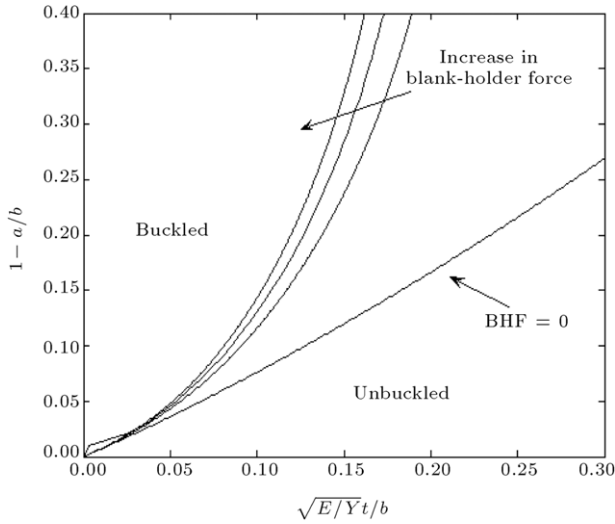


Figure 9: Effect of BHF on onset of plastic wrinkling.

Figures 8 and 9 show the effect of blankholder force on the number of wrinkles and onset of the wrinkling. For a constant value of $(1 - \frac{a}{b})$, it is observed that when the blankholder force rises, the number of waves increases and the onset of wrinkling postpones.

4.2. Thin plate with large deflection

Eq. (1) in this case becomes:

$$\begin{aligned}
 F(u, v, w) &= \frac{1}{2} \int_0^{2\pi} \int_a^b \left[\frac{t^3}{12} L_{ijkl}^{ep} \kappa_{ij} \kappa_{kl} \right. \\
 &\quad \left. + t L_{ijkl}^{ep} \varepsilon_{ij}^0 \varepsilon_{kl}^0 + t \sigma_{ij} w_{,i} w_{,j} \right] r dr d\theta \\
 &\quad + \frac{1}{2} K (w_{\max}^2 + u_{\max}^2 + v_{\max}^2) \\
 &= \frac{1}{2} \int_0^{2\pi} \int_a^b \frac{t^3}{12} L_{ijkl}^{ep} \kappa_{ij} \kappa_{kl} r dr d\theta \\
 &\quad + \frac{1}{2} \int_0^{2\pi} \int_a^b t L_{ijkl}^{ep} \varepsilon_{ij}^0 \varepsilon_{kl}^0 r dr d\theta
 \end{aligned}$$

$$\begin{aligned}
 &+ \frac{1}{2} \int_0^{2\pi} \int_a^b t \sigma_{ij} w_{,i} w_{,j} r dr d\theta \\
 &+ \frac{1}{2} K (w_{\max}^2 + u_{\max}^2 + v_{\max}^2). \quad (62)
 \end{aligned}$$

The displacement, u and v , can be assumed as Eq. (28). Since the maximum deflections are:

$$\begin{cases} u_{\max} = dr \cos n\theta \Big|_{\theta=0}^{r=b} = db, \\ v_{\max} = er \sin n\theta \Big|_{\theta=\frac{\pi}{2n}}^{r=b} = eb. \end{cases} \quad (63)$$

Hence:

$$\begin{cases} \frac{1}{2} K u_{\max}^2 = \frac{S}{2\pi(b^2 - a^2)} d^2 b^2 = \frac{1}{2\pi} \frac{S d^2}{(1 - m^2)}, \\ \frac{1}{2} K v_{\max}^2 = \frac{S}{2\pi(b^2 - a^2)} e^2 b^2 = \frac{1}{2\pi} \frac{S e^2}{(1 - m^2)}. \end{cases} \quad (64)$$

Then the energy stored in the spring-type blankholder is:

$$\begin{aligned}
 \frac{1}{2} K (w_{\max}^2 + u_{\max}^2 + v_{\max}^2) &= \frac{2}{\pi} S \frac{1 - m}{1 + m} c^2 \\
 &+ \frac{1}{2\pi} \frac{S}{(1 - m^2)} (d^2 + e^2). \quad (65)
 \end{aligned}$$

Finally, the functional becomes:

$$\begin{aligned}
 F &= \frac{1}{2} \int_0^{2\pi} \int_a^b \left\{ \frac{t^3}{12} \left[L_{1111}^{ep} \left(\frac{\partial^2 w}{\partial r^2} \right)^2 \right. \right. \\
 &\quad + 2L_{1122}^{ep} \left(\frac{\partial^2 w}{\partial r^2} \right) \left(\frac{1}{r} \frac{\partial w}{\partial r} + \frac{1}{r^2} \frac{\partial^2 w}{\partial \theta^2} \right) \\
 &\quad + L_{2222}^{ep} \left(\frac{1}{r} \frac{\partial w}{\partial r} + \frac{1}{r^2} \frac{\partial^2 w}{\partial \theta^2} \right)^2 \\
 &\quad \left. \left. + 4L_{1212}^{ep} \left(\frac{1}{r} \frac{\partial^2 w}{\partial r \partial \theta} - \frac{1}{r^2} \frac{\partial w}{\partial \theta} \right)^2 \right] \right\} r dr d\theta \\
 &+ \frac{1}{2} \int_0^{2\pi} \int_a^b \left\{ t \left[L_{1111}^{ep} \left(\frac{\partial u}{\partial r} \right)^2 \right. \right. \\
 &\quad + 2L_{1122}^{ep} \left(\frac{\partial u}{\partial r} \right) \left(\frac{u}{r} + \frac{1}{r} \frac{\partial v}{\partial \theta} \right) + L_{2222}^{ep} \left(\frac{u}{r} + \frac{1}{r} \frac{\partial v}{\partial \theta} \right)^2 \\
 &\quad \left. \left. + L_{1212}^{ep} \left(\frac{1}{r} \frac{\partial u}{\partial \theta} + \frac{\partial v}{\partial \theta} - \frac{v}{r} \right)^2 \right] \right\} r dr d\theta \\
 &+ \frac{1}{2} \int_0^{2\pi} \int_a^b \left\{ t \left[\sigma_r \left(\frac{\partial w}{\partial r} \right)^2 + \sigma_\theta \left(\frac{1}{r} \frac{\partial w}{\partial \theta} \right)^2 \right] \right\} r dr d\theta \\
 &+ \frac{2}{\pi} S \frac{1 - m}{1 + m} c^2 + \frac{1}{2\pi} \frac{S}{(1 - m^2)} (d^2 + e^2). \quad (66)
 \end{aligned}$$

It is enough now to calculate only the second integration, because the first and third are exactly the same as in the small deflection case in Eq. (52).

$$\begin{aligned}
 F &= \frac{t^3 c^2 E \pi}{96(1 - \nu^2)} G^{ep}(m, n, \nu) \\
 &+ \frac{\pi t E b^2}{8(1 - \nu^2)} \{ Q^{ep}(m, n, \nu) d^2 + R^{ep}(m, n, \nu) e^2 \\
 &\quad + S^{ep}(m, n, \nu) e^2 \} + \frac{t \pi b^2 c^2 Y}{8} H^{ep}(m, n) \\
 &+ \frac{2}{\pi} S \frac{1 - m}{1 + m} c^2 + \frac{1}{2\pi} \frac{S}{(1 - m^2)} (d^2 + e^2). \quad (67)
 \end{aligned}$$

The critical condition for plastic buckling is $F = 0$. Now we have:

$$F = \begin{Bmatrix} c & d & e \end{Bmatrix} \begin{bmatrix} M_{11} & 0 & 0 \\ 0 & M_{22} & M_{23} \\ 0 & M_{32} & M_{33} \end{bmatrix} \begin{Bmatrix} c \\ d \\ e \end{Bmatrix}, \quad (68)$$

where:

$$\begin{cases} M_{11} = \frac{t^3 E \pi}{96(1-\nu^2)} G^{ep}(m, n, \nu) + \frac{\pi b^2 t Y}{8} H^{ep}(m, n) \\ \quad + \frac{2}{\pi} S \frac{1-m}{1+m}, \\ M_{22} = \frac{\pi t E b^2}{8(1-\nu^2)} Q^{ep}(m, n, \nu) + \frac{1}{2\pi} \frac{S}{(1-m^2)}, \\ M_{23} = M_{32} = \frac{1}{2} \frac{\pi t E b^2}{8(1-\nu^2)} R^{ep}(m, n, \nu), \\ M_{33} = \frac{\pi t E b^2}{8(1-\nu^2)} S^{ep}(m, n, \nu) + \frac{1}{2\pi} \frac{S}{(1-m^2)}. \end{cases} \quad (69)$$

The first and the second conditions for occurring wrinkling lead to conditions similar to those of small and large deflections in elastic and plastic wrinkling without blankholders. It is observed that the results for the critical number of waves and the critical load are exactly the same as the ones obtained from the small deflection theory when the nonlinear terms in stretching tensor, ε_{ij}^0 , are neglected.

5. Discussion

Figure 7 shows a comparison between the current results and those from Geckeler and Senior. As mentioned earlier, Geckeler's result [3] is a good approximation for small values of $1 - \frac{a}{b}$, i.e. narrow flanges, but its error rises as the width of the flange increases. Moreover, Yu's results [8] give curved lines for different n 's, and the current obtained curve is the envelope of those lines. In the current study, more exact expressions for $n_{critical}$, $p_{critical}$ and $Y_{critical}$ for each case (elastic-plastic wrinkling and without/with blankholder) could be obtained without any approximations or interpolations (Figure 5). It has to be mentioned that the derivation of L_{ijkl}^{ep} is carried out based on the Tresca yield criterion, which makes the components of the stiffness matrix independent of the deviatoric stresses. It simplifies the analytical study, while the results are still in good agreement with the experimental results. However, using the von Mises yield criterion causes the dependency of L_{ijkl}^{ep} on the nonlinear distribution of deviatoric stresses and therefore the explicit integral does not exist. In this case, some numerical approximations are required to obtain those critical values that need more calculation time, however, the results are nearly the same as in the current study. The dependency of L_{ijkl}^{ep} to deviatoric stresses for perfectly plastic material in von Mises yield criterion for a plane stress problem can be obtained as: (also check [25,26]):

$$L_{ijkl}^{ep} = \begin{bmatrix} \frac{ES_{22}^2}{S_{11}^2 + S_{22}^2 + 2\nu S_{11}S_{22}} & \frac{-ES_{11}S_{22}}{S_{11}^2 + S_{22}^2 + 2\nu S_{11}S_{22}} & 0 \\ \frac{-ES_{11}S_{22}}{S_{11}^2 + S_{22}^2 + 2\nu S_{11}S_{22}} & \frac{ES_{11}^2}{S_{11}^2 + S_{22}^2 + 2\nu S_{11}S_{22}} & 0 \\ 0 & 0 & \frac{E}{2(1+\nu)} \end{bmatrix}, \quad (70)$$

where S_{ij} are the deviatoric stresses. It can be proved that using the large deflection theory without considering nonlinear terms, whose effects are too small, according to experimental results has no effect on critical values if the displacement fields of u , v and w satisfy the boundary conditions. For instance, if they are assumed as:

$$\begin{cases} w = cf_1(r)g_1(\theta), \\ u = df_2(r)g_2(\theta), \\ v = ef_3(r)g_3(\theta). \end{cases} \quad (71)$$

For example:

$$\begin{cases} w(r, \theta) = c(r-a)(1 + \cos n\theta), \\ u(r, \theta) = dr^k \cos n\theta \\ \text{or } u(r, \theta) = dr^k(1 + \cos n\theta), \\ v(r, \theta) = er^k \sin n\theta \\ \text{or } v(r, \theta) = er^k(1 + \sin n\theta), \end{cases} \quad (72)$$

where c , d and e are constants and k is a positive integer. It is assumed that the functions of $f_1(r)g_1(\theta)$, $f_2(r)g_2(\theta)$ and $f_3(r)g_3(\theta)$ satisfy the kinematical boundary conditions for w , u and v (at $r = au$, $v \neq 0$; $w = 0$; $w(r, \theta)$; $u(r, \theta)$ and $v(r, \theta) \geq 0$ for $a \leq r \leq b$).

After substituting these terms into Functional 1 and integration, it is found that:

$$F = \begin{Bmatrix} c & d & e \end{Bmatrix} \begin{bmatrix} M_{11} & 0 & 0 \\ 0 & M_{22} & M_{23} \\ 0 & M_{23} & M_{33} \end{bmatrix} \begin{Bmatrix} c \\ d \\ e \end{Bmatrix}. \quad (73)$$

Now the condition of:

$$\text{Det}(M_{ij}) = M_{11}(M_{22}M_{33} - M_{23}^2) = 0,$$

yields to $M_{11} = 0$, which is exactly the same condition as in the small deflection theory.

During shell analysis, also if nonlinear terms are neglected, we have:

$$\varepsilon_{ij}^0 = \frac{1}{2}(u_{i,j} + u_{j,i}) + b_{ij}w,$$

where b_{ij} is the curvature tensor of the middle surface in the pre-buckling state, which is zero for plates. Because of the term of $b_{ij}w$, the functional in shells becomes [15–17]:

$$F = \begin{Bmatrix} c & d & e \end{Bmatrix} \begin{bmatrix} M_{11} & M_{12} & M_{13} \\ M_{21} & M_{22} & M_{23} \\ M_{31} & M_{32} & M_{33} \end{bmatrix} \begin{Bmatrix} c \\ d \\ e \end{Bmatrix} = u^T Mu, \quad (74)$$

where M_{ij} is a symmetric matrix. In this case, the effect of large deflection can be seen in the following two conditions:

$$\begin{cases} F = 0 & \text{or } \text{Det}(M_{ij}) = 0, \\ \frac{\partial F}{\partial n} = 0 & \text{or } \frac{\partial [\text{Det}(M_{ij})]}{\partial n} = 0. \end{cases} \quad (75)$$

Therefore, the small and large deflection theories have the same results.

Finally, it is observed from Figures 10 and 11 that the aluminum wrinkles under lower loads than steel for the same value of $(1 - \frac{a}{b})$ for elastic and plastic wrinkling problems.

6. Conclusions

The elastic and plastic wrinkling of flanges in deep drawing has been studied analytically using a bifurcation functional and Tresca yield criterion. For a large width of flange, the analytical solution could determine more exact values, which are closer

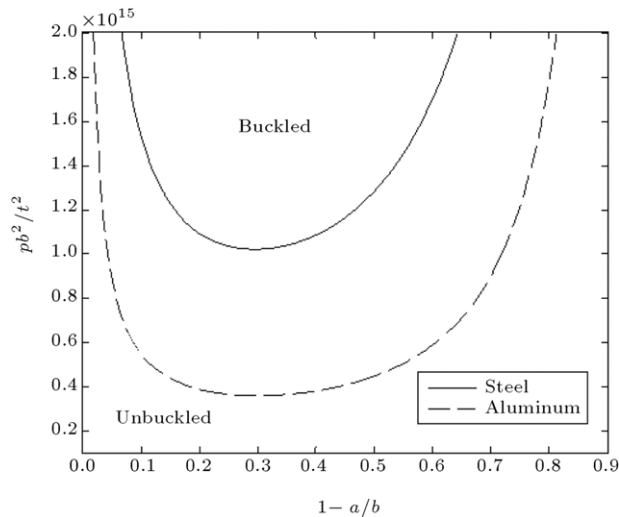


Figure 10: Comparison between onset of wrinkling for steel and aluminum.

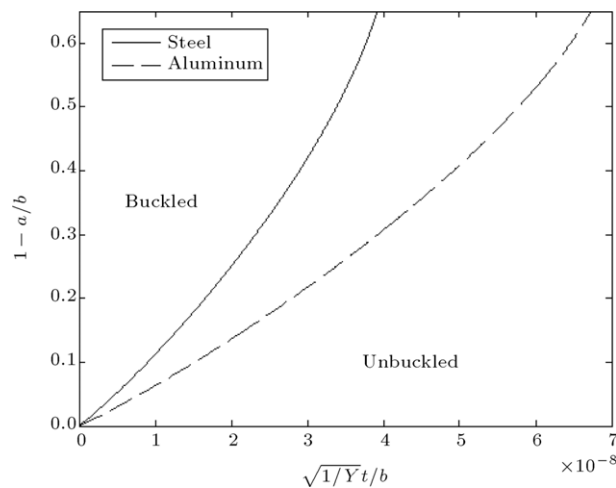


Figure 11: Onset of wrinkling for steel and aluminum.

to experimental results. The influence of a blankholder upon wrinkling and on the number of waves could be successfully predicted. It was found that considering the large deflection theory, with neglecting nonlinear terms, has no effect on predicting the onset of wrinkling.

References

- [1] Sivasankaran, S., et al. "Modelling of wrinkling in deep drawing of different grades of annealed commercially pure aluminum sheets when drawn through a conical die using artificial neural network", *Materials and Design*, 30, pp. 3193–3205 (2009).
- [2] Chu, E. and Xu, Y. "An elasto-plastic analysis of flange wrinkling in deep drawing process", *Journal of Mechanics and Physics of Solids*, 43, pp. 1421–1440 (2001).
- [3] Geckeler, J.W. "Plastische Knicken der Wandung von Hohlzylindern und einige andern Falguger Scheinungen", *Zeitschrift für Angewandte Mathematik und Mechanik*, 8, pp. 341–352 (1928).
- [4] Esser, H. and Arend, H. "Die Tiefzieh Prüfung von Blechen", *Archiv für das Eisenhüttenwesen*, 14, pp. 223–239 (1940).
- [5] Baldwin, W.M. and Howald, T.S. "Folding in the cupping operation", *Transactions of American Society for Metals*, 38, pp. 757–788 (1947).
- [6] Senior, B.W. "Flange wrinkling in deep-drawing operation", *Journal of Mechanics and Physics of Solids*, 4, pp. 235–246 (1956).
- [7] Alexander, J.M. "An appraisal of the theory of deep-drawing", *Metallurgical Reviews*, 5(19), pp. 349–411 (1960).
- [8] Yu, T.X. and Johnson, W. "The buckling of annular plates in relation to deep-drawing process", *International Journal of Mechanical Sciences*, 24, pp. 175–188 (1982).
- [9] Zhang, L.C. and Yu, T.X. "The plastic wrinkling of an annular plate under uniform tension on its inner edge", *International Journal of Solids Structures*, 24(5), pp. 497–503 (1988).
- [10] Yossifon, S. and Tirosh, J. "The maximum drawing ratio in hydroforming processes", *Journal of Engineering for Industry*, 112, pp. 47–56 (1990).
- [11] Ravindra, K.S. and Dixit, P.M. "Prediction of flange wrinkling in deep drawing process using bifurcation criterion", *Journal of Manufacturing Process*, 12, pp. 19–29 (2010).
- [12] Wang, X.W. "A new computational method for wrinkling analysis of gossamer space structures", *International Journal of Solids and Structures*, 46, pp. 1516–1526 (2009).
- [13] Hutchinson, J.W. "Plastic buckling", *Advances in Applied Mechanics*, 67, pp. 14–16 (1974).
- [14] Hutchinson, J.W. and Neale, K.W. "Wrinkling of curved thin sheet metal", *Proceedings of International Symposium on Plastic Instability*, Paris, France, pp. 1841–1914 (1985).
- [15] Hill, R. "A general theory of uniqueness and stability in elastic/plastic solids", *Journal of Mechanics and Physics of Solids*, 6, pp. 236–249 (1958).
- [16] Hill, R. "Bifurcation and uniqueness in nonlinear mechanics of continua", *Society of Industrial Applied Mathematics*, pp. 236–274 (1961).
- [17] Magalhaes, J.P.De. and Ferron, C.G. "Wrinkling prediction in the deep-drawing process of anisotropic metal sheets", *Journal of Materials and Processing Technology*, 128, pp. 178–190 (2002).
- [18] Magalhaes, J.P.De. and Ferron, C.G. "Wrinkling of anisotropic metal sheets under deep-drawing analytical and numerical study", *Journal of Materials Processing Technology*, 155–156, pp. 1604–1610 (2004).
- [19] Wang, C., et al. "Wrinkling criterion for anisotropic shell with compound curvatures in sheet forming", *International Journal of Mechanical Sciences*, 36, pp. 945–960 (1994).
- [20] Timoshenko, S. and Woinowsky, K., *Theory of Plates and Shells*, McGraw-Hill, New York (1961).
- [21] Reddy, J.N., *Energy Principles and Variation Methods in Applied Mechanics*, John Wiley & Sons (2002).
- [22] Tomita, Y. "Bounding approach to the bifurcation point of annular plates with non-associated flow rule subjected to uniform tension at their outer edges", *International Journal of Plasticity*, 4, pp. 251–263 (1988).
- [23] Tomita, Y. and Shindo, A. "On the bifurcation and post-bifurcation behavior of thick circular elastic-plastic tubes under lateral pressure", *International Journal of Plasticity*, 35, pp. 207–219 (1982).
- [24] Chen, W.F. and Zhang, H., *Structural Plasticity Theory, Problems, and CAE Software*, Springer-Verlag, New York (1936).
- [25] Khan, A. and Hung, S., *Continuum Theory of Plasticity*, John Wiley & Sons (1995).
- [26] Chakrabarty, J., *Theory of Plasticity*, McGraw-Hill Book Company, New York (2006).
- [27] Hill, R., *The Mathematical Theory of Plasticity*, Oxford University Press, New York (1950).

Mehran Kадkhodayan received his B.S. and M.S. degrees in Solid Mechanics from Tehran University in 1985 and 1987, respectively. He obtained his Ph.D. degree from Sydney University, Australia, in 1996. He is currently working in the Department of Mechanical Engineering at Ferdowsi University of Mashhad. He has published about 48 conference papers and 27 journal papers. His main areas of interest include Plasticity and Sheet Metal Forming.

Farzad Moayyedyan obtained his B.S. and M.S. degrees in Solid Mechanics from Azad University and Ferdowsi University in Mashhad in 2006 and 2008, respectively. He is currently a Ph.D. student at Ferdowsi University. He has published three conference papers and two journal papers.